1990

Noise Source Identification in Semi-Hermetic Twin-Screw Compressors

R. W. Andrews
Purdue University

J. D. Jones
Purdue University

NOISE SOURCE IDENTIFICATION IN SEMI-HERMETIC TWIN-SCREW COMPRESSORS

Andrews, R.W. and Jones, J.D.

The Ray W. Herrick Laboratories, School of Mechanical Engineering
Purdue University, West Lafayette, IN 47907 USA

ABSTRACT

The sound radiation characteristics of a semi-hermetic twin-screw compressor were studied while operating under controlled laboratory conditions at the Ray W. Herrick Laboratories of Purdue University. A fully-condensing load stand was designed to allow the 70 ton chiller system to be operated at the three standard loading capacities of the compressor. The load stand was operator controlled and was used to vary individual compressor operating parameters for sensitivity studies. The two-microphone cross-spectral intensity technique was used to evaluate the radiated sound field for a variety of compressor operating conditions. The majority of the acoustic radiation occurred at the first five harmonics of the fundamental screw frequency of refrigerant gas discharge from the rotors (300 Hz). The compressor sound power levels were highest at part load conditions (50% capacity). Discharge gas pulsations and rotor vibration were the primary noise generating mechanisms. At full load (100% capacity) and the higher part load condition (75% capacity), gas pulsation was the primary noise generating mechanism. For the smaller part load condition (50% capacity), the overall pulsation effect was much the same as for the higher capacities. However, the decrease in the mass flow rate at 50% capacity promoted chatter between the twin helical rotors during the compression process, making rotor chatter an important noise generating mechanism at this capacity.

INTRODUCTION

Recent interest in screw compressors has been motivated by the potential of these compressors in commercial refrigeration and liquid-chilling applications. It is known that screw compressors are a cost-effective alternative to typical refrigeration compressors because of their low noise and vibration, high reliability, and durability [1]. Yet though screw compressors are viewed favorably when compared to typical refrigeration compressors, little is known about their sound and vibration characteristics. Thus, further improvements in the noise and vibration characteristics of screw compressors is difficult without a fundamental understanding of their noise generating mechanisms.

The identification of the principle sound sources and noise generating mechanisms of twin-screw compressors was the objective of this study. This paper documents the results of external sound field and internal refrigerant gas pulsation measurements of the compressor. Using a controllable test setup that enabled repeatable measurements of the system parameters, the effect on the compressor's radiated sound field with respect to a change in the compressor's operating condition was evaluated. This method identified the contributions of the most significant noise generating mechanisms to the radiated sound field. The design and construction of the compressor load stand is described in a

companion paper [2].

TEST COMPRESSOR AND LOAD STAND

The test compressor used for this study was a semi-hermetic twin-screw type capable of operation at three standard capacities (50%, 75% and 100%). The maximum cooling capacity was 70 tons (844 kBtu/h) at 100% capacity. Figure 1 shows a schematic diagram of the test compressor.

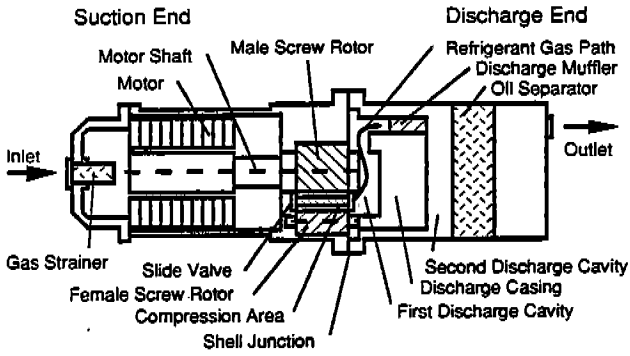

Figure 1. Cutaway Top View of Twin-Screw Compressor

A twin-screw compressor accomplishes refrigerant gas compression via the motor-induced rotation of two specially designed, intermeshing helical rotors. Figure 2 shows a pair of helical screw rotors. Before compression begins, refrigerant gas enters the suction side of the compressor in a superheated state, and passes through and cools the hermetic motor. The suction process begins as a lobe (on the male screw rotor) and flute (on the female screw rotor) come to a specific angle of rotor rotation. At that angle, a tube on each screw rotor opens to the suction port. The tubes are formed due to the recessed portions of the screw rotors. As screw rotor rotation proceeds, both tubes fill with refrigerant gas. The tubes are open on the suction side until the rotation of the screw rotors closes them to the suction port. Slightly further rotation causes the twin tubes to join and form a single chamber. When the chamber is unrolled onto a two-dimensional surface, it can be visualized to form a V during the compression process, with the tubes functioning as the legs of the V. At the bottom of the V is the intersection of the tubes (the interfacial seal line), which moves to the discharge end as the screw rotors rotate. The advance of the interfacial seal line during screw rotor rotation reduces the size of the chamber and consequently compresses the refrigerant gas.

Eventually the orientation of the rotors is such that the chamber opens into the radial and axial discharge ports, and the gas discharges into the first discharge cavity. In addition to the seal provided by the interfacial seal line, the compression chamber is sealed during compression by the discharge casing and the rotor housing during compression. The rotor housing provides radial constraint on the chamber, while the discharge casing provides axial constraint on the discharge end of the chamber. Also, refrigerant oil is fed into the

chamber by a difference between the oil reservior pressure and the pressure on the suction side. The oil lubricates and seals the rotors to minimize leakage from the chamber.

The test compressor has a five lobe male rotor and a six flute female rotor. This lobe-flute orientation produces five discharges of refrigerant gas for every rotor rotation. Thus, the test compressor's motor speed of approximately 60 Hz produces a fundamental screw frequency (FSF) of refrigerant gas discharge of approximately 300 Hz. In the test compressor, the male rotor is directly driven by the motor through a shaft, so the male rotor's rotation speed is equal to the motor's rotation speed.

The operating capacity of the test compressor was varied using a slide

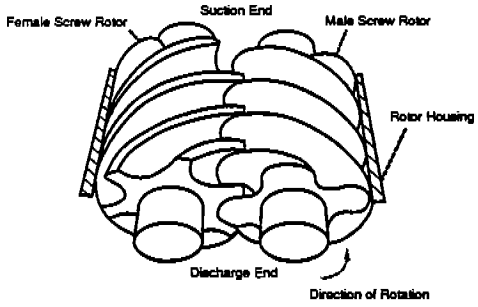

Figure 2. Twin Helical Screw Rotors

valve. When the slide valve was moved to uncover an area on the suction side of the rotors, refrigerant gas was bypassed back to the suction side. Increased gas bypass decreased the mass flow rate and consequently reduced the capacity. The slide valve was actuated by a pressure difference acting on a piston in the compressor discharge casing. The position of the slide valve was varied in three discrete steps using operator-controlled solenoid valves.

Control of the compressor and its operating condition was accomplished through the load stand [2]. For the purposes of the study, a fully-condensing load stand was selected because it provided the necessary stability for acoustic measurements. The operator was able to use the load stand to select the exact loading condition desired and keep the system at a steady-state condition for an indefinite period of time. The load stand also allowed the compressor suction and discharge pressures to be varied while all other operating parameters were maintained at constant levels, providing the ability for sensitivity testing, which was used to describe the effect of the operating pressure condition on the radiated sound field.

COMPRESSOR EFFICIENCY AT PART LOADING

Since twin-screw compressors are operated at a variety of loading conditions, a capacity control system is used to increase the part load efficiency. For the test compressor, the capacity was varied using a slide valve. The position of the slide valve controlled not only the refrigerant flow rate, but also the ratio of the volume of the refrigerant gas chamber at the start of compression to that in the chamber at the instant discharge began. This volume ratio Vi varied for each capacity. The value of Vi defined the optimum pressure ratio of operation by

$$(P_{discharge}/P_{suction})_{optimum} = (Vi)^{\gamma} \qquad (1)$$

where P is absolute pressure, and γ is the ratio of the specific heats of the refrigerant gas. Thus, given the suction pressure and Vi, the discharge pressure at which the efficiency is maximized (power requirement is minimized) could be determined.

Operation at a non-optimal pressure ratio causes inefficiencies in the compression process [3]. If the operating pressure ratio is lower than the optimum ratio, an overpressure condition results (i.e., the chamber pressure is higher than the pressure in the first discharge cavity). Conversely, an operating pressure ratio higher than the optimum pressure ratio is termed an underpressure condition (i.e., the chamber pressure is lower than the pressure in the first discharge cavity). Both conditions cause the compressor to waste power in the cycle compensating for the difference in pressure, and thus will produce discharge pressure pulsations. The gas pulsations occur at harmonics of the FSF.

For the test compressor, the Vi ratio was a built-in component of the design and varied only with the loading condition. Vi varied with the slide valve position as shown in Figures 3 and 4. Figure 3 shows the internal components which control capacity change, and Figure 4 shows an approximate operating curve relating the Vi ratio to the operating capacity. The operating Vi ratio of the compressor was governed by the discharge ports. If the radial port was the first to open, the radial Vi controlled the optimum pressure ratio. Conversely, if the axial port was the first to open, the axial Vi controlled the optimum pressure ratio. The axial Vi varied only due to the amount of refrigerant gas bypassed. As the slide valve moved linearly to the discharge end, both capacity and the axial Vi decreased linearly. Conversely, the radial Vi varied nonlinearly due to both the amount of refrigerant gas bypassed and the size of the radial discharge opening. As the slide valve initially moved to the discharge side from the 100% capacity, the radial Vi decreased because the suction volume (the numerator of Vi) decreased at a faster rate than the discharge volume (the denominator of Vi). At a specific capacity, the radial Vi reached a minimum. As the capacity further decreased, the radial Vi increased as the suction volume approached a constant and the discharge volume decreased rapidly. At 50% capacity, the radial port almost closed off and the radial Vi tended to infinity, allowing the axial port to define the operating Vi.

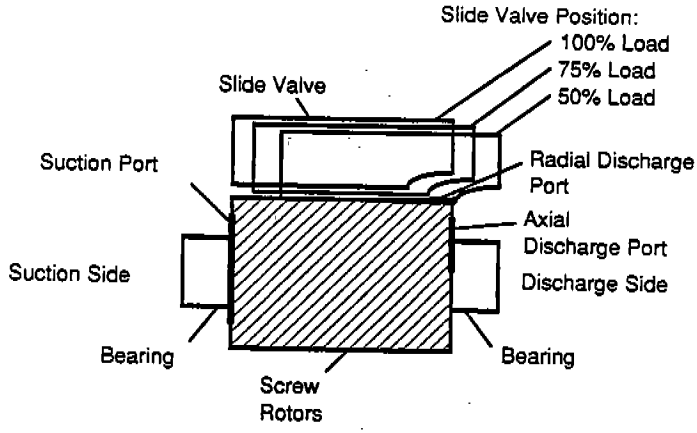

Figure 3. Capacity Control of the Test Compressor

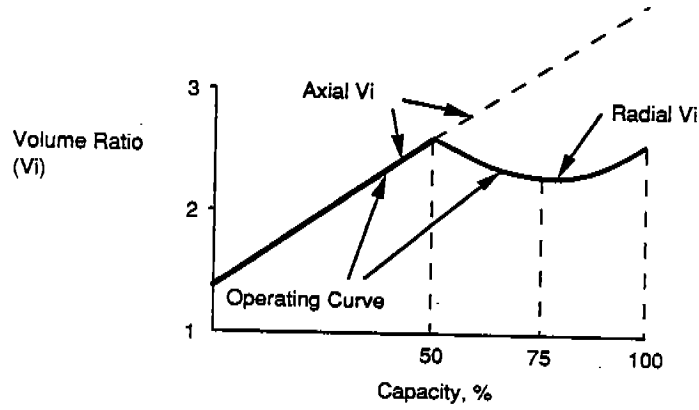

Figure 4. Operating Curve of the Test Compressor

SUMMARY OF EXPERIMENTS

The gas pressure pulsations caused by overpressure or underpressure conditions were measured in the first discharge cavity of the system shown in Figure 1. A dynamic pressure transducer and a signal analyzer were used to obtain the pulsation signal in the frequency domain. Pulsation levels were measured for each of the three loading conditions at steady-state over a broad range of discharge pressures. The variation in discharge pressure allowed operation of the compressor in both overpressure and underpressure conditions for all three capacities.

The sound intensity measurements were performed using the two-microphone sound intensity technique over a 99 point grid around the compressor. The conformal grid was a cylindrical shape, composed of 11 rows along the compressor length and nine circumferential rings around the compressor. Each point was equally spaced and established an equal area on the grid. The grid was designed such that each measurement point was approximately six inches from the compressor surface, keeping measurements in the acoustic near field to identify the sound radiation characteristics of the compressor. No measuring points were placed beneath the compressor because of space interference due to the compressor supports, which prevented the entire sound power of the compressor from being measured. The sound intensity was calculated using a Fast Fourier Transform analyzer with a 4 Hz bandwidth over the frequency range of 125-3200 Hz. The sound power was calculated by an area summation of intensity. During compressor operation, the sound power was measured over a broad range of discharge pressures at each capacity. Thus, the pulsation levels and radiated sound levels were measured for the same operating conditions. The system parameters were measured during the tests to verify the steady-state condition.

RESULTS AND DISCUSSION

Figures 5, 6, and 7 show the sound power spectra over the measured frequency range for compressor capacities of 50%, 75%, and 100%, respectively. The operating condition was a suction pressure of 68 psig and a discharge pressure of 211 psig. The figures were generated from the 99 sound intensity spectra measured over the grid surface at each capacity. For all three standard capacities, the sound power spectra were dominated by the first four harmonics of the FSF. The harmonics of the FSF are labelled in the figures. Similar results were observed in an earlier experimental study of twin-screw compressors [4]. The source of the tones at the FSF can be attributable to either gas pulsations and/or rotor vibrations. Rotor vibrations are associated with the impact and subsequent vibration of the twin helical rotors as they mesh during operation. Unfortunately, since both gas pulsations and rotor vibration generate tones at harmonics of the FSF, they are perfectly coherent. Thus, the contribution due to each source cannot be easily ascertained. Nevertheless, the results of the sound power spectra shown in Figures 5, 6, and 7 can lend some insight into the principle sound sources at each individual capacity.

At 50% capacity, the first four harmonics of the FSF clearly stand out with higher peak levels than that at 75% or 100% capacity. Also, there is a significant contribution from the accumulated effect of a series of harmonics spaced approximately 60 Hz apart below 1 kHz. These harmonics can be seen to some degree at 75% capacity, but are not present at 100% capacity. Because the harmonics occur at approximately 60 Hz intervals, the sound generating mechanism is coherent with the motor speed. The principle source of the 60 Hz harmonic tones appears to be rotor vibration, as gas pulsations occur only at the harmonics of the FSF (300, 600, 900 Hz, etc.). Operation of the compressor at lower capacities allows for more play between the rotors, which consequently tends to promote rotor vibration. Thus, the 60 Hz harmonics are probably due to a slight imperfection in one or more of the male rotor lobes. Such lobe imperfections are known to create harmonics of the male rotor speed [4]. In contrast, at 75% and 100% capacity, the 60 Hz harmonics are less prominent in the radiated sound spectra. Thus, rotor vibration at these higher capacities is likely reduced, diminishing the significance of this sound generating mechanism.

This reduction in rotor vibration is likely due to the added buffer (or cushion) provided by high refrigerant flow rates at higher capacities.

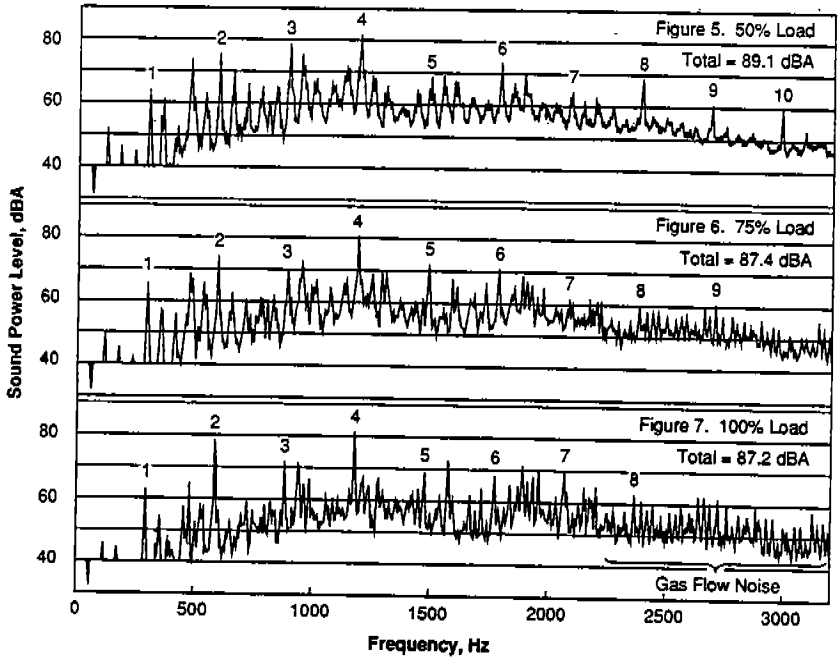

The results of the pulsation tests for varying discharge pressures are shown in Figures 8, 10, and 12 for operating capacities of 50%, 75%, and 100%, respectively. The pulsation levels are shown for the overall spectrum (summation of 0-3200 Hz) and the first two harmonics of the FSF (300 and 600 Hz). The pulsation levels for each capacity are unique, and the trend for the overall level is reflected by the trends of the first two harmonics of the FSF (the dominant components by 10-15 dBA of the pulsation signal). For each capacity, the pulsation levels reach a minimum at a specific discharge pressure. An estimate of the optimal discharge pressure to minimize gas pulsations can be obtained from equation (1) using a suction pressure of 83 psia and a γ of 1.3. These values corresponded to the test conditions. Table 1 compares the location of the pulsation minima between prediction and measurement. The estimates are proportionally correct but differ because the prediction does not account for compression leakage effects. Accounting for leakage effects will tend to reduce the predicted pulsation minima, thus bringing the prediction and measured values into closer agreement.

Table 1. Discharge Pressures for Pulsation Minima

Capacity (%)	Prediction (psig)	Measurement (psig)
50	274	225
75	253	188
100	310	252

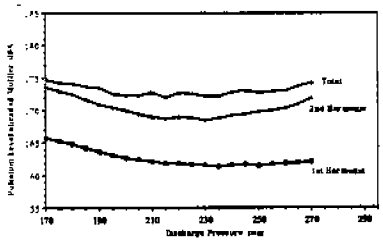

Figure 8. Gas Pulsations at 50% Capacity

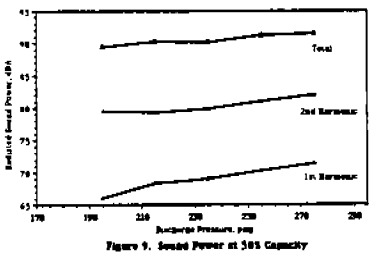

Figure 9. Sound Power at 50% Capacity

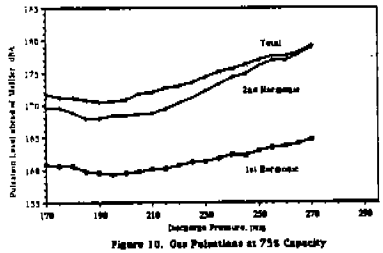

Figure 10. Gas Pulsations at 75% Capacity

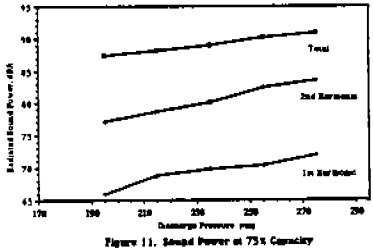

Figure 11. Sound Power at 75% Capacity

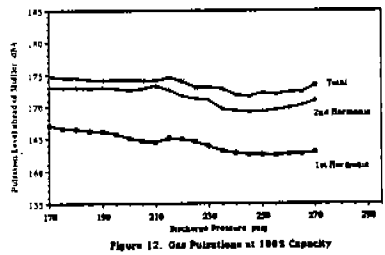

Figure 12. Gas Pulsations at 100% Capacity

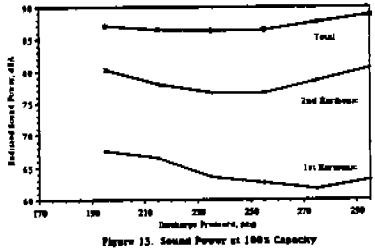

Figure 13. Sound Power at 100% Capacity

At the optimum pressure ratio computed from equation (1), the pulsation level would theoretically be zero, since there should be no difference in pressure between that in the trapped refrigerant gas chamber and that in the first discharge cavity. Yet the pulsation level never reaches a value even remotely near zero for the range of discharge pressures measured. In fact, all capacities have a measured pulsation reduction at the optimum discharge pressure of only approximately 6-15 dB. The limited reduction in the discharge pulsations is due to the added compression of the refrigerant gas chambers after the discharge port opens during the compression process, i.e., the discharge port does not open quickly enough to prevent further compression after opening. Thus, the additional compression causes a portion of the refrigerant gas to discharge into the discharge cavity at a pressure higher than that of the cavity, creating an overpressure condition and subsequently a gas pulsation.

The sound power levels as a function of discharge pressure are shown in Figures 9, 11, and 13 for capacities of 50%, 75%, and 100%, respectively. The power levels are shown for the overall spectrum (125-3200 Hz) and the first two harmonics of the FSF, generated by a summation of the spectra of the 99 near field grid measurement points. The sound power levels for each capacity are unique, and the trend for the overall level is reflected in the trends of the first two harmonics of the FSF. For the range of discharge pressures measured

at 50% capacity, there does not appear to be a direct correlation between the trends of the sound power levels and the pulsation levels (especially the first harmonic), suggesting that another sound generating mechanism (rotor chatter) is more significant. In contrast, at 75% capacity, the trends in the sound power and pulsation levels are in closer agreement over the measured range. Similarly, at 100% capacity the trends correlate very well, with both levels having minima at approximately the same discharge pressure.

CONCLUSIONS

The principle sound generating mechanism for twin-screw compressors at 100% and 75% capacity is gas pulsations, which are directly related to inefficiencies in the compression process. Conversely, for the 50% capacity condition the pulsation levels are essentially equal to those at full capacity, but the radiated sound levels are noticeably higher. The increased sound levels are due to rotor noise (chatter) associated with the twin-rotor interaction under partial capacity conditions, and suspected imperfections in the male rotor which occur at harmonics of the male rotor speed (60 Hz). The chatter is promoted by the decrease in mass flow rate at lower capacity, which allows the rotors to interact with less of a refrigerant gas cushion. At higher capacities (75% and 100% capacity), the radiated sound field was quieter because the added capacity reduced the rotor vibrations.

At any one of the three capacities, the added compression of the refrigerant gas chamber after the discharge port opens results in only a limited reduction in the discharge pulsations at the optimum pressure ratio. Attempts to operate the compressor at slightly underpressure conditions can help with this problem but cannot eliminate it. These results clearly indicate the importance of discharge port design when modifying a screw compressor to reduce discharge pulsations.

ACKNOWLEDGEMENTS

The authors wish to thank United Technologies Carrier for their support of this research. The technical assistance of John Jabobs, Jack O'Brien, and Erric Heitmann of Carrier is gratefully acknowledged. The authors also wish to thank Kwang-Lu Koai and Dr. Werner Soedel for their contributions to this work through many insightful discussions.

REFERENCES

[1] Ernst, S., Advantages of Screw Compressors. Heat Piping Air Cond (59) n 11

[2] Andrews, Jones, et. al., Development of an Operator Controlled Compressor Load Stand for Liquid-Chiller Systems. In *Proceedings of 1990 International Compressor Engineering Conference at Purdue*. Purdue University, West Lafayette, IN, 1990.

[3] O'Brien, J., Built In Volume Ratio (Vi) as it Relates to Screw Compressors - Twin and Single. Carlyle Compressor report. Carlyle Compressor Co., Syracuse, NY, 1987.

[4] Fujiwara, A., & Sakurai, N., Experimental Analysis of Screw Compressor Noise and Vibration. In *Proceedings of 1986 International Compressor Engineering Conference at Purdue*. Purdue University, West Lafayette, IN, 1986.